

Synthesis and Properties of Functionalized Polybenzimidazoles for High-Temperature PEMFCs

Seonghan Yu[†] and Brian C. Benicewicz^{*‡}

Department of Chemistry and Chemical Biology, New York State Center for Polymer Synthesis, Rensselaer Polytechnic Institute, 110 Eighth Street, Troy, New York 12110. [†]Current address: BASF Fuel Cell, Inc., 39 Veronica Ave., Somerset, NJ 08873. [‡]Current address: Department of Chemistry and Biochemistry, USC NanoCenter, University of South Carolina, Columbia, SC 29208

Received July 18, 2009; Revised Manuscript Received October 14, 2009

ABSTRACT: Polybenzimidazole (PBI) derivatives having dihydroxy functional groups (poly(2,2'-(dihydroxy-1,4-phenylene)5,5'-bibenzimidazole), 2OH-PBI) were successfully synthesized in poly(phosphoric acid) (PPA). The 2OH-PBI polymer underwent cross-linking reactions during the polymerization in poly(phosphoric acid) via the formation of phosphate bridges between the hydroxy groups of the polymer backbone. Gelation of the polymer solution during the polymerization was avoided by conducting the polymerization at relatively low monomer concentrations. The 2OH-PBI membranes showed higher proton conductivity compared to the unfunctionalized analogue, poly(2,2'-(1,4-phenylene)5,5'-bibenzimidazole) (*para*-PBI) membranes. Carefully controlled experiments were conducted to analyze separately the effects of both phosphoric acid doping level and polymer structure on the proton conductivity. Both polymer structure and phosphoric acid doping level were important determinants of membrane proton conductivity. The fuel cell performance of 2OH-PBI membranes was evaluated in membrane electrode assemblies (MEAs) using standard platinum (Pt) on carbon-based electrodes and Pt alloy on carbon-based cathode electrodes. The higher proton conductivity of the 2OH-PBI membranes did not result in increases in fuel cell performance when tested on Pt electrodes. However, Pt alloy cathode catalysts resulted in an increase in fuel cell performance. The fuel cell performance of 2OH-PBI membranes with Pt alloy cathode catalyst was 0.69 V at 0.2 A/cm² and 0.49 A/cm² at 0.6 V at 180 °C under H₂/air operation and ambient pressure.

Introduction

Phosphoric acid-doped polybenzimidazole (PBI)-based membranes are the most prominent candidates for high-temperature polymer electrolyte membrane fuel cells (PEMFC). In the 1990s, researchers at Case Western Reserve University first used phosphoric acid-doped poly(2,2'-(1,3-phenylene)-5,5'-bibenzimidazole) (*meta*-PBI, Figure 1a) as an electrolyte membrane for fuel cell applications.¹ Although other groups also showed that phosphoric acid-doped PBIs are promising candidates for high-temperature PEM fuel cells, *meta*-PBI and poly(2,5-benzimidazole) (AB-PBI) (Figure 1b) have been mainly studied due to commercial availability of the polymer or monomer. Another reason that *meta*-PBI and AB-PBI are widely studied is their solubility in organic solvents such as *N,N*-dimethylacetamide (DMAc) for film casting. However, a new PBI gel membrane preparation process, called the poly(phosphoric acid) (PPA) process, was recently developed and broadened the PBI selection for PBI gel membranes.² Polymer rigidity and “phosphophilicity” (solubility or affinity for phosphoric acid) were two major factors that determine the membrane properties for high-temperature fuel cell applications. Homopolymers and copolymers of AB-PBI, *para*-PBI (Figure 1c), and pyridine-based PBI³ (PPBI, Figure 1d) were synthesized and investigated over the past several years. It was reported previously that rigid-rod polymers having nitrogen heterocycles and hydroxy groups can form strong hydrogen bonds between the polymer chains and create network structures.^{4–7} Additional work has disclosed the formation of cross-links in such structures via phosphate bridges when the

reactions were conducted in poly(phosphoric acid).⁸ In this paper, PBI membranes containing dihydroxy groups (2OH-PBI, Figure 1e) were prepared by the PPA process and investigated in terms of their chemical structure, polymer and membrane properties, and fuel cell performance.

Experimental Section

Materials. TAB (3,3',4,4'-tetraaminobiphenyl, polymerization grade) was obtained from Celanese Ventures, GmbH. Terephthalic acid (TA, 99+%) was purchased from Amoco. Both were used as received. 2,5-Dihydroxyterephthalic acid (2OH-TA, 98%) was purchased from Aldrich and purified by recrystallization in an ethanol and water mixture (EtOH: water = 3:2). *o*-Phenylenediamine (98%) for model compound synthesis was purchased from Acros Organics and used without further purification. Poly(phosphoric acid) (PPA, 115%) was used as supplied from Aldrich and FMC Corp.

Polymer and Membrane Preparation. *Synthesis of 2OH-PBI Homopolymer.* TAB (3,3',4,4'-tetraaminobiphenyl) (6.730 g, 31.41 mmol), 2,5-dihydroxyterephthalic acid (2OH-TA) (6.223 g, 31.41 mmol), and 400 g of poly(phosphoric acid) were placed in a 500 mL round-bottom flask equipped with an overhead stirrer and nitrogen gas purging. The solution was stirred at 140 °C for 3 h, and the temperature was raised to 195 °C. The polymerization was conducted for 13 h at 195 °C. Monomer concentration at the beginning of the reaction was 3.14 wt % and yielded a 2.6 wt % final polymer concentration. After the final stage of polymerization, the temperature was raised to 220 °C to lower the solution viscosity and aid the membrane casting process. The yield of polymer was nearly quantitative.

*Corresponding author. E-mail: benice@sc.edu.

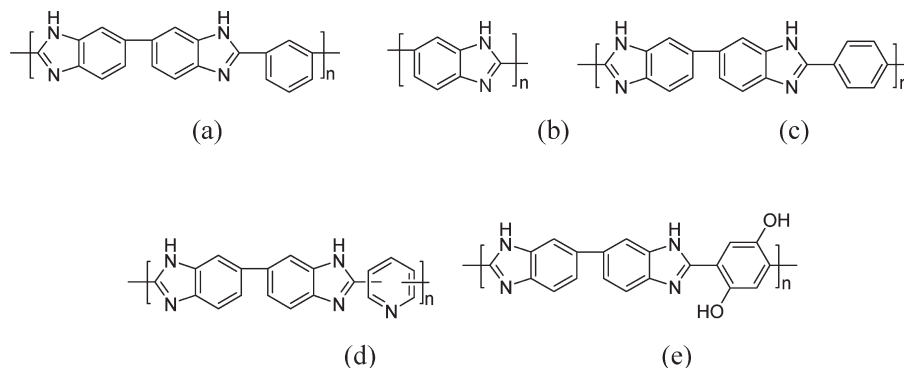


Figure 1. Chemical structures of various polybenzimidazoles (PBIs): (a) *meta*-PBI [poly(2,2'-(1,3-phenylene) 5,5'-bibenzimidazole)], (b) AB-PBI [poly(2,5-benzimidazole)], (c) *para*-PBI [poly(2,2'-(1,4-phenylene) 5,5'-bibenzimidazole)], (d) PPBI [pyridine-based PBIs], and (e) 2OH-PBI [poly(2,2'-(2,5-dihydroxy-1,4-phenylene) 5,5'-bibenzimidazole)].

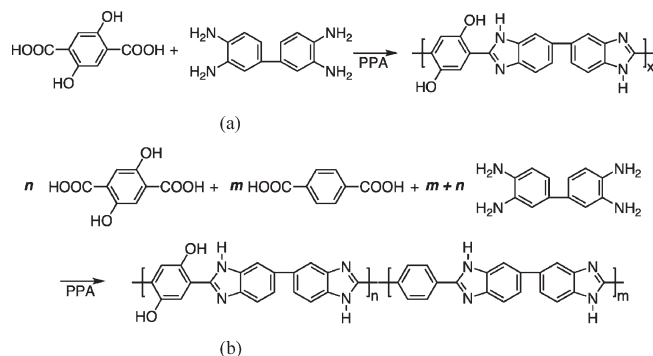
Table 1. Reagent Ratios and Monomer/Polymer Concentrations Used for the Polymerization of 2OH-PBI Homopolymer and Copolymers^a

2OH-PBI/ <i>para</i> -PBI	TAB, g (mol)	2OH-TA, g (mol)	TA, g (mol)	PPA, g	monomer concentration, wt %	polymer concentration, wt %
100/0	6.703 (0.0314)	6.223 (0.0314)		400.1	3.14	2.60
75/25	6.890 (0.0322)	4.778 (0.0241)	1.336 (0.00804)	400.0	3.15	2.60
50/50	7.050 (0.0329)	3.259 (0.0165)	2.733 (0.0165)	400.7	3.15	2.59
25/75	6.650 (0.0310)	1.537 (0.0078)	3.867 (0.0233)	401.7	2.91	2.39

^a 2OH-PBI [poly(2,2'-(2,5-dihydroxy-1,4-phenylene) 5,5'-bibenzimidazole)], *para*-PBI [poly(2,2'-(1,4-phenylene) 5,5'-bibenzimidazole)], TAB [3,3',4,4'-tetraaminobiphenyl], 2OH-TA [2,5-dihydroxyterephthalic], TA [terephthalic acid], PPA [poly(phosphoric acid)].

Scheme 1. Synthetic Scheme of Homopolymer and Copolymers:

(a) 2OH-PBI [Poly(2,2'-(2,5-dihydroxy-1,4-phenylene) 5,5'-bibenzimidazole)] Homopolymer; (b) Random Copolymers of 2OH-PBI and *para*-PBI [Poly(2,2'-(1,4-phenylene) 5,5'-bibenzimidazole)]



Synthesis of Copolymers of 2OH-PBI and *para*-PBI. Copolymers were also synthesized as described above with a final polymerization step at 195 °C for 13 h. Initial monomer concentrations were adjusted to ~3.0 wt %. The solutions were cast at a polymer concentration of ~2.5 wt %. The detailed monomer and polymer concentrations for typical homopolymer and copolymer polymerizations are summarized in Table 1.

Film Casting and Membrane Electrode Assembly (MEA) Fabrication. When polymerization was complete, the polymer solution was poured onto clean glass plates and cast at a controlled gate thickness using a Gardner blade. The temperature of the casting solution was 220 °C, and the casting thickness was 380 μ m. The films on the plates were moved to a humidity-controlled chamber where the poly(phosphoric acid) in the membranes was hydrolyzed to phosphoric acid in an environment of 55% RH (27 \pm 1 °C) for 24 h.

Although hydrolysis in a humidity-controlled chamber was the most common membrane preparation process, there can be an additional soaking process to control the acid doping level of the membranes. Phosphoric acid solution baths were prepared by mixing *o*-phosphoric acid and water in a glass tray to make various concentrations (wt %) of phosphoric acid such as 70, 50,

and 30 wt % phosphoric acid solutions for acid doping level control experiments. A strip (10 cm \times 30 cm) of PBI membrane was soaked in 1500 mL of each phosphoric acid solution for 16 h at room temperature. After 16 h of immersion in the solution, the excess liquid on the membrane was removed and the membranes were stored in sealed plastic bags for further study.

A membrane electrode assembly (MEA) was fabricated by placing a membrane between two electrodes and hot pressing for 30 s at 140 °C using 4 N/mm² of pressure. Both anode and cathode electrodes were commercially available E-TEK electrodes. Platinum (Pt) catalyst (1 mg/cm², 30% on Vulcan XC-72) was used for anode electrodes. For cathode electrodes, two different types of catalysts were used to evaluate the effect of catalyst type: one was 1 mg/cm² of platinum (Pt) catalyst (30% on Vulcan XC-72), and another was 1 mg/cm² of Pt alloy catalyst (30% on Vulcan XC-72). Single stack fuel cells were built and used for fuel cell performance measurement, and the active area of the fuel cell was 45.15 cm².

Synthesis of Oligomers and Model Compounds. The model compound of 2OH-PBI [2,5-bis(2-benzimidazolyl)hydroquinone] was synthesized in poly(phosphoric acid) with 2,5-dihydroxyterephthalic acid and an excess of *o*-phenylenediamine. A mixture of 2,5-dihydroxyterephthalic acid (6.093 g, 30.75 mmol), *o*-phenylenediamine (7.244 g, 66.80 mmol), and 300 g of poly(phosphoric acid) (PPA) in a 500 mL round-bottom flask was heated to 195 °C and stirred in a nitrogen atmosphere using an overhead mechanical stirrer. After 13 h, the solution was poured into 4000 mL of water to precipitate a dark yellow solid. The crude product was collected by filtration, neutralized in 1000 mL of water with ammonium hydroxide, and washed three times with boiling water to remove salts. The soluble impurities were removed by Soxhlet extraction with ethanol for 24 h. The solid was dried in a vacuum oven at 130 °C overnight. This crude product is an oligomeric mixture with phosphate bridges as shown in Figure 5. The yield was 14.99 g, 145% (theoretical yield, 10.366 g), due to phosphate bridges between 2OH-PBI model compounds.

Pure 2OH-PBI model compound which does not have phosphate bridges was prepared by employing an additional reaction to hydrolyze the phosphate bridges. The crude product (14.098 g) and 0.24 g of sodium hydroxide (0.02 M) were placed in 300 mL of a dimethyl sulfoxide (DMSO) and water mixture (DMSO:water

(w/w) = 95:5) and heated at 85 °C for 12 h. The solution was poured into 4000 mL of distilled water, filtered, and dried in a vacuum oven at 100 °C overnight (9.557 g). The product was purified as follows: 5.157 g of base-treated sample was dissolved in 250 mL of DMSO by refluxing for an hour, the solution was poured into 3500 mL of water, and the filtered solid was washed in 2000 mL of boiling water. The pale yellow powder was dried in a vacuum oven overnight at 100 °C (4.420 g, overall yield, 79%), $T_m > 400$ °C. ^1H NMR (500 MHz, $\text{DMSO}-d_6$): δ 7.32 (m, 4H, benzimidazole ring), 7.62 (d, 2H, benzimidazole ring), 7.75 (d, 2H, benzimidazole ring), 7.79 (s, 2H, aromatic ring *ortho*-OH). FT-IR (KBr): 3316 s (hydrogen-bonded —OH and —NH groups), 3060 w (aromatic C—H stretch), 1558 m, 1502 s, 1360 m, 837 m, 723 s cm^{-1} .

Characterization Techniques. NMR and IR spectra were recorded using a 500 MHz NMR (Varian 500) and a Bio-Rad FT 3000 FTIR, respectively. Acid doping levels and membrane composition were determined by titration with 0.1 N sodium hydroxide solution using an automatic titrator, 716 DMS Titrino (Metrohm Co. Ltd.).³ Proton conductivity was measured by a four-probe ac impedance method with a Zahner IM6e in the frequency range of 1 Hz–100 kHz.³

Results and Discussion

Polymer Synthesis. Dihydroxy-PBI (2OH-PBI) and copolymers with *para*-PBI were synthesized in poly(phosphoric acid) (PPA) using the PPA process as described previously.² The typical polymerization procedure contains a polymer solution dilution step with phosphoric acid after 13 h of polymerization at 195 °C to adjust casting viscosity. However, 2OH-PBI was much less soluble in phosphoric acid than *para*-PBI, and polymer precipitation occurred when adding phosphoric acid into the polymer solution at the end of the polymerization. The cross-linked structure of 2OH-PBI may contribute to this behavior and will be discussed later. A typical monomer concentration of 3.5 wt % resulted in a polymer solution which was too viscous to obtain a good film quality. To overcome the problems caused by the low solubility of 2OH-PBI in PPA/PA mixed solutions, the polymerization conditions for 2OH-PBI were modified from the typical PBI polymerization conditions. In the modified polymerization conditions, the initial monomer concentration was lowered to ~3.0 wt % (from 3.5 wt %) to obtain a polymer content of ~2.5 wt %, and the phosphoric acid dilution step was eliminated. With the lower monomer and polymer concentrations, the polymer solution could be cast without phosphoric acid dilution after 13 h of polymerization. Strong, brown membranes were obtained after hydrolysis of poly(phosphoric acid) to phosphoric acid in a humidity-controlled chamber. Three compositions of copolymers (25%, 50%, and 75% of 2OH-PBI with *para*-PBI) and 2OH-PBI homopolymer were synthesized by the same procedure to investigate the effect of copolymer composition on polymer and membrane properties.

Membrane Characterization. *Polymer Structure.* Dried polymer powders were placed into concentrated sulfuric acid at a concentration of 0.2 g/dL for inherent viscosity measurements. However, the polymers were not fully dissolved even after shaking for 3 days. In comparison, *para*-PBI dissolved in 24 h at the same concentration. A possible reason for the low solubility is the formation of a polymer network formed by intermolecular hydrogen bonding. Poly-{2,6-diimidazo[4,5-*b*:4',5'-*e*]pyridinylene-1,4-(2,5-dihydroxy)phenylene} (PIPD) (Figure 2a) has a similar chemical structure to 2OH-PBI. It was reported that the PIPD polymer in the solid state can form extensive intermolecular hydrogen-bonded structures.^{5,6,9} Although intramolecular O—H...N bonds can be

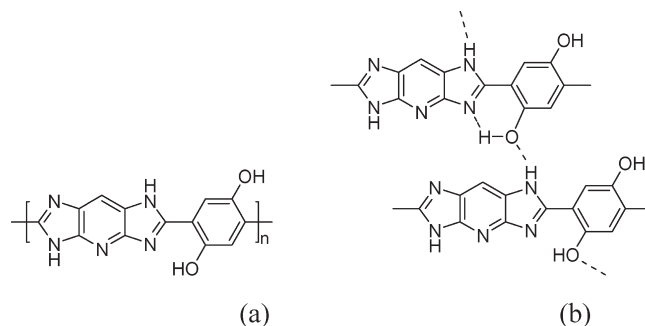


Figure 2. (a) Chemical structure of PIPD [poly(2,6-diimidazo[4,5-*b*:4',5'-*e*]pyridinylene-1,4-(2,5-dihydroxy)phenylene) and (b) suggested arrangement of hydrogen bonds in PIPD.

formed, intermolecular N—H...O bonds were also formed as suggested in Figure 2b,⁶ and the intermolecular hydrogen-bonding energy per PIPD repeat unit was reported to be -22.6 kcal/mol⁹ or -20.8 kcal/mol.⁶ Another possible explanation for the low polymer solubility is cross-linking of polymer chains through phosphate bridges. The esterification of hydroxy groups by phosphoric acid is well documented in the literature.¹⁰ The phosphoric acid esters can be formed by heating a mixture of hydroxy compounds with phosphoric acid to temperatures above 100 °C. The reaction of hydroxy compounds with poly(phosphoric acid)s also gives esters of phosphoric acid by the progressive cleavage of the phosphorus–oxygen–phosphorus anhydride link. Dihydroxy compounds in 115% poly(phosphoric acid) are expected to form phosphate linkages at the polymerization conditions for 2OH-PBI, which is 13 h at 195 °C.⁸ The formation of a cross-linked structure may explain the insolubility of polymers in phosphoric acid and sulfuric acid. Figure 3 (top) shows the suggested structure of the polymer which is cross-linked through phosphate bridges. The linear 2OH-PBI chains connected by phosphate bridges would not be as long as *para*-PBI chains because the viscosity of the final polymer solution of 2OH-PBI was controlled to have a similar solution viscosity to that of *para*-PBI. If individual linear 2OH-PBI chains connected by phosphate bridges were long, it would be impossible to cast membrane films due to uncontrollably high viscosity and low solubility.

The suggested polymer structure in Figure 3 (top) would contain the relatively shorter linear 2OH-PBI chains cross-linked by phosphate bridges. To confirm the cross-linked polymer structure, experiments were conducted to selectively cleave the phosphate bridges. Phosphate esters can be hydrolyzed under basic conditions.¹⁰ Normally the inherent viscosities of PBIs are measured by dissolving them in concentrated sulfuric acid (96% H_2SO_4). As mentioned previously, 2OH-PBI was not fully dissolved in concentrated sulfuric acid even after shaking for a week at a concentration of 0.2 g/dL, which implied a cross-linked structure. Thus, 2OH-PBI was hydrolyzed in a DMSO/water mixture with 0.02 M of sodium hydroxide as described in the literature.¹¹ The inherent viscosity of hydrolyzed 2OH-PBI was subsequently measured in concentrated sulfuric acid (0.2 g/dL) at 30.0 °C and was found to be 0.74 dL/g. Typically the inherent viscosity of *para*-PBI is 3.0–3.5 dL/g when polymerized under similar conditions.^{2,3} As indicated by the solubility behavior and inherent viscosity measurements of base-treated 2OH-PBI, 2OH-PBI is believed to be cross-linked through phosphoric acid ester bridges. The hydrolysis of phosphate bridges in 2OH-PBIs as shown in Figure 3 may have been limited by the low solubility of 2OH-PBI polymer in the solvent mixture of 95% DMSO and 5% water, and

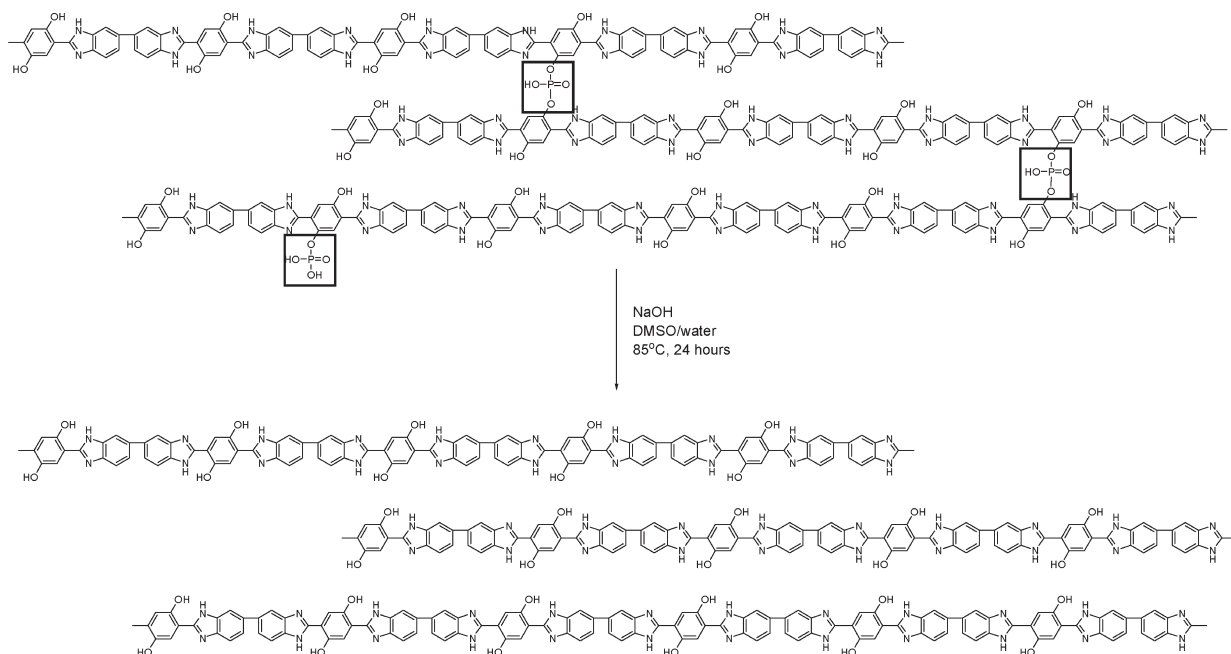


Figure 3. Hydrolysis of phosphate bridges of the cross-linked 2OH-PBI [poly(2,2'-(2,5-dihydroxy-1,4-phenylene) 5,5'-bibenzimidazole)] under basic conditions.

thus, it is hard to confirm that all of the phosphate bridges were hydrolyzed. However, the low solubility of the as-prepared 2OH-PBI in PPA, the insolubility of the as-prepared 2OH-PBI in sulfuric acid, the increased solubility of the polymer after mild base treatment, and the low inherent viscosity of the polymer after base treatment are all consistent with the cross-linked structure proposed here.

2OH-PBI/*para*-PBI random copolymers also exhibited low solubility in concentrated sulfuric acid at a concentration of 0.2 g/dL in concentrated sulfuric acid for inherent viscosity measurements. If the onset of gelation (loss of stirring) during the polymerization is dependent on the cross-linking through phosphate bridges, copolymers are also expected to have longer linear chains connected through fewer phosphate bridges because they have fewer hydroxy groups in the polymer chains. As a result, the copolymers showed much lower solubility in the DMSO/water solvent mixture used for hydrolysis. Even after several days of exposure to the hydrolysis reaction conditions, the copolymer membranes in the reaction flask maintained their film shape. Thus, the copolymers could not be dissolved in sulfuric acid or hydrolyzed in basic solution. Because quantitative information on the copolymer structure was not obtained, it could only be postulated from these observations that copolymers also have a cross-linked structure and the length of linear chains connected by phosphate bridges increased as the 2OH-PBI content in the copolymers decreased due to fewer hydroxy groups. This type of cross-linked structure would maintain low solubility in sulfuric acid and resist dissolution in the DMSO/water hydrolysis reaction mixture.

A model compound study was conducted to confirm the phosphate linkage formation between hydroxy groups of the PBI and phosphoric acid or poly(phosphoric acid). The model compound of 2OH-PBI, as shown in Figure 4, was prepared by the reaction of 2OH-TA with an excess of *o*-phenylenediamine in PPA at 195 °C for 13 h. It was expected that the phosphate linkages would be formed during the synthesis of the model compounds. Figure 5 shows some possible examples of 2OH-PBI model compounds containing phosphate

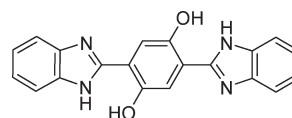


Figure 4. Chemical structure of the model compound 2,5-bis(2-benzimidazolyl)hydroquinone.

linkages. For 2OH-PBI model compounds having two hydroxyl groups, it was expected that a mixture of monomers, dimers, trimers, etc., would be formed. Product identification would be further complicated because each oligomer species can have 0, 1, or 2 phosphoric acid ester groups. Thus, the reaction was conducted as described earlier and washed thoroughly to remove residual phosphoric acid, and the isolated product was subjected to FT-IR analysis.

FT-IR spectra of the 2OH-PBI oligomers and model compound were compared to confirm the formation of phosphate bridges. Figure 6a shows an FT-IR spectrum of the model compound of 2OH-PBI after base treatment (Figure 4), and Figure 6b is that of the mixture of the oligomers having phosphoric acid ester groups prior to base treatment (Figure 5). The spectrum in Figure 6 exhibits characteristic peaks from the model compound: broad and strong peak at 3316 cm^{-1} for the hydrogen-bonded hydroxyl group and N-H stretch, peak at 3060 cm^{-1} for aromatic C-H stretch, and peaks at 1557, 1504, 1360, 837, and 723 cm^{-1} as described in the literature.¹² Figure 6 shows broad additional peaks at 1240–1190 and 995–850 cm^{-1} from the aromatic phosphate (P–O–C stretch)¹³ which confirms the formation of phosphoric acid esters and phosphate bridges between 2OH-PBI model compounds. Weak peaks in Figure 6 at 1620 cm^{-1} (open-chain imino, —C=N—) and at 3238 cm^{-1} (aromatic primary amine, NH stretch) imply the existence of the intermediate before ring closure.

Acid Doping Levels and Proton Conductivity. Acid doping levels of the homopolymer and copolymer membranes were determined by titration with 0.1 N sodium hydroxide solutions. Figure 7 shows the proton conductivity curves of the 2OH-PBI and *para*-PBI membranes. Both 2OH-PBI and

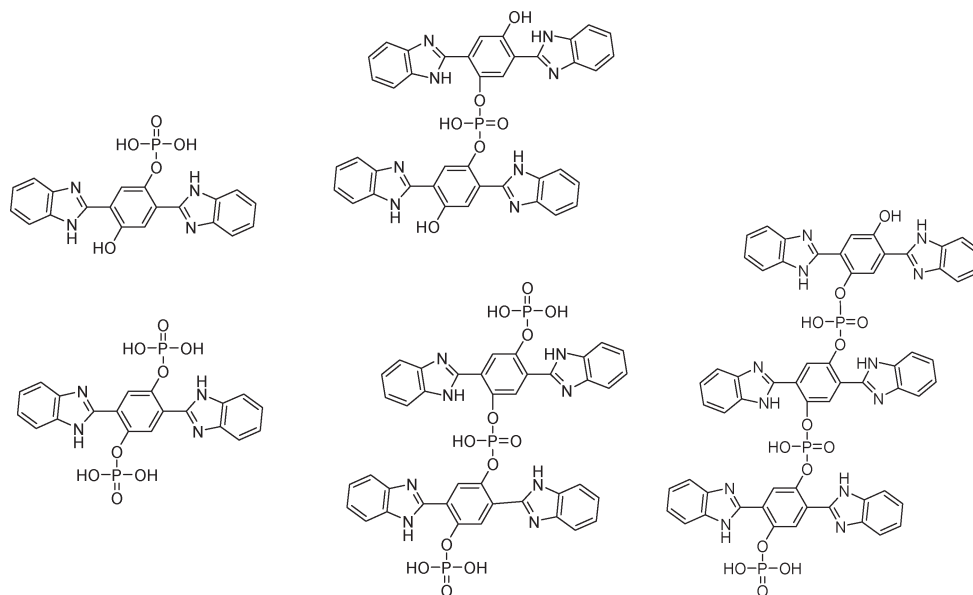


Figure 5. Chemical structure of 2OH-PBI [poly(2,2'-(2,5-dihydroxy-1,4-phenylene) 5,5'-bibenzimidazole)] oligomers with phosphoric acid ester linkages.

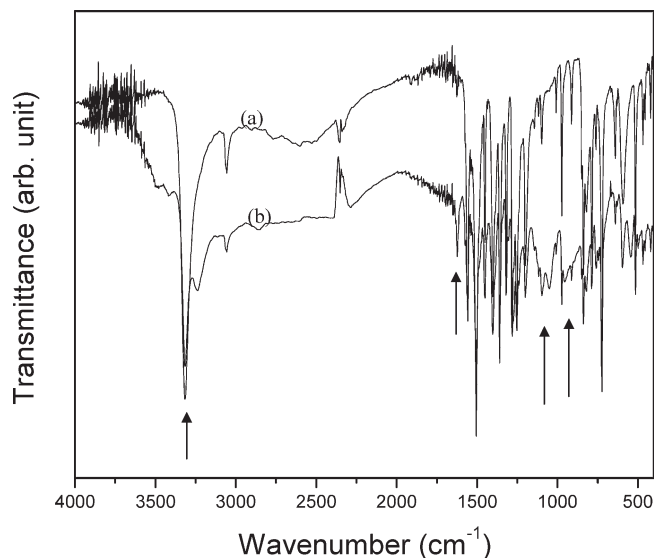


Figure 6. FT-IR spectra of 2OH-PBI [poly(2,2'-(2,5-dihydroxy-1,4-phenylene) 5,5'-bibenzimidazole)] oligomers and model compound: (a) hydrolyzed model compound and (b) oligomers after reaction (imidization).

para-PBI membranes were prepared under the same hydrolysis conditions in a humidity-controlled chamber at 55% RH (27 ± 1 °C) for 24 h. However, the proton conductivity of 2OH-PBI was higher than *para*-PBI membranes over the entire temperature range from room temperature to 180 °C. For example, the proton conductivity of the 2OH-PBI membrane at 160 °C was 0.35 S/cm while the proton conductivity of *para*-PBI membrane was about 0.27 S/cm at the same temperature (see also Table 2). The proton conductivity of the 2OH-PBI membrane was as high as 0.43 S/cm with an acid doping level of 28.3 PA/repeat unit in some batches of polymerization. From the data in Table 2, it might appear that the membrane proton conductivity increased with the increasing content of 2OH-PBI repeating units in the homopolymer or copolymers. Although the 2OH-PBI membrane had a higher acid doping level when processed under the same hydrolysis conditions than *para*-PBI, the dependence of acid

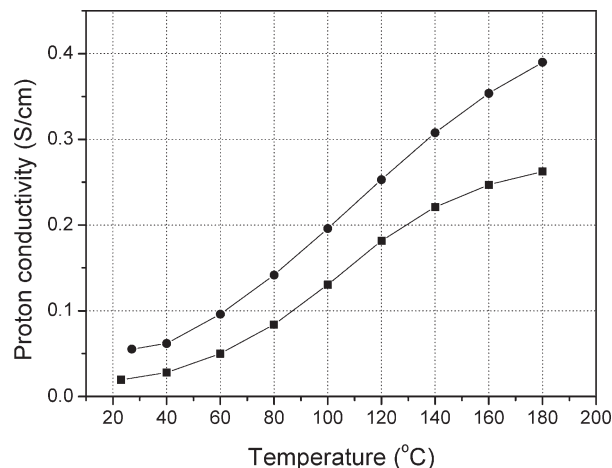


Figure 7. Proton conductivities of phosphoric acid-doped 2OH-PBI [poly(2,2'-(2,5-dihydroxy-1,4-phenylene) 5,5'-bibenzimidazole)] (circles) and *para*-PBI [poly(2,2'-(1,4-phenylene) 5,5'-bibenzimidazole)] (squares) membranes.

doping level and proton conductivity on copolymer composition is not easily correlated.

A new set of experiments was designed to investigate the effects of phosphoric acid doping level on proton conductivity for both 2OH-PBI and *para*-PBI homopolymer membranes. Previous work had found that the acid content of membranes can be adjusted and controlled by soaking membranes in phosphoric acid baths of different concentrations.¹⁴ As shown in Table 2, the PBI membranes consisted of 5–6 wt % of polymer solid and 94–95 wt % of liquid. The liquid was a mixture of phosphoric acid and water, and the composition of liquid in the membrane will reach equilibrium with the phosphoric acid bath concentration by soaking the PBI membranes in acid bath. Thus, the acid doping level of the membrane can be adjusted and controlled by changing the phosphoric acid bath concentration. Because the membrane is not soluble and is stable to phosphoric acid under these conditions, the membranes are substantially equivalent, and the only variable among them is the phosphoric acid doping level. The strips of *para*-PBI and 2OH-PBI (10 cm × 30 cm)

Table 2. Summary of Acid Doping Level and Membrane Composition of Homopolymer and Copolymer Membranes of 2OH-PBI and *para*-PBI^a

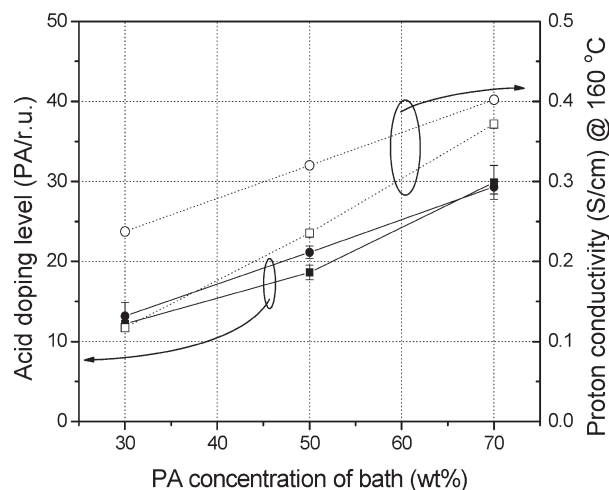
2OH-PBI/ <i>para</i> -PBI	acid doping level (PA/r.u.)	proton conductivity at 160 °C (S/cm)	membrane composition (wt %)		
			solid	PA	water
100/0	25.4	0.35	5.31	38.70	55.99
75/25	22.1	0.31	5.86	37.79	56.35
50/50	20.9	0.33	5.91	37.41	56.68
25/75	23.1	0.27	5.48	39.04	55.48
0/100	19.3	0.27	6.35	38.84	54.81

^a 2OH-PBI [poly(2,2'-(2,5-dihydroxy-1,4-phenylene) 5,5'-bibenzimidazole)], *para*-PBI [poly(2,2'-(1,4-phenylene) 5,5'-bibenzimidazole)], PA/r.u. [moles of phosphoric acid per mole repeat unit].

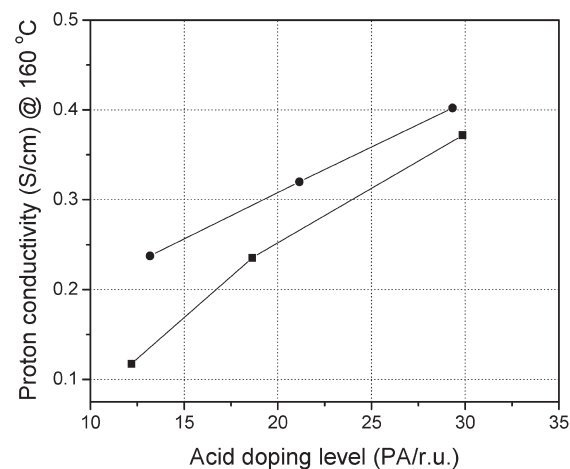
hydrolyzed in the humidity-controlled chamber were soaked in 30, 50, and 70 wt % phosphoric acid baths at room temperature for 16 h to adjust the acid doping level. After removal of the PBI membranes from the acid baths, the membranes were characterized by measuring their phosphoric acid doping levels and proton conductivity.

Figure 8 shows the results of these experiments and the relationships among chemical structure, phosphoric concentration of the bath, acid doping level, and proton conductivity of the membranes at 160 °C. The membranes soaked in the baths of varying phosphoric acid concentration had similar acid doping levels (Figure 8, filled symbols). Only minor differences in acid doping levels caused by molecular weight of the polymer repeat unit and variation of polymer solid content were observed in each set of films. However, the proton conductivity of 2OH-PBI membrane at 160 °C was higher than that of *para*-PBI membrane soaked in the identical phosphoric acid baths (Figure 8, unfilled symbols). After converting the titration data into the molar ratio of phosphoric acid per polymer repeat unit (PA/repeat unit), Figure 8 clearly shows that 2OH-PBI membranes exhibit higher proton conductivity than *para*-PBI membranes over a wide range of acid doping levels. We conclude that the higher proton conductivity of 2OH-PBI membrane is derived from its chemical structure or morphology differences induced by the chemical structure and not simply from the higher acid doping levels of the membrane. It is generally believed that high phosphoric acid doping levels are necessary to obtain high proton conductivity. Although generally true, the results show that the chemical structure of PBI membranes is also an important factor in determining the proton conductivity of the membranes.

The results of phosphoric acid doping level adjustment experiments in Figure 8 show that the chemical structure of PBI membrane is an important factor in determining proton conductivity, and hydroxy functional groups may play an important role to increase the proton conductivity. Thus, both polymer chemical structure and phosphoric acid doping level must be considered when evaluating the proton conductivity of PBI membranes. The copolymers having 25%, 50%, and 75% 2OH-PBI content and the 2OH-PBI homopolymer were prepared and soaked in a 70 wt % phosphoric acid bath for 16 h. Analysis of the membranes showed that the amount of phosphoric acid of the liquid in the membranes was about 67 wt %. Figure 9 shows the proton conductivities and phosphoric acid contents of 2OH-PBI containing polymers at 160 °C as a function of 2OH-PBI content measured at three different places within a single strip of membrane for each composition. The polymers with the higher 2OH-PBI content showed higher proton conductivity at equivalent phosphoric acid doping levels. Again, this



(a)



(b)

Figure 8. (a) Effect of phosphoric acid bath concentration on acid doping level (filled symbols) and proton conductivity (unfilled symbols), for 2OH-PBI [poly(2,2'-(2,5-dihydroxy-1,4-phenylene) 5,5'-bibenzimidazole)] (circles) and *para*-PBI [poly(2,2'-(1,4-phenylene) 5,5'-bibenzimidazole)] (squares) membranes, (b) proton conductivity of 2OH-PBI (circles) and *para*-PBI (squares) membranes at different acid doping levels [PA/r.u. = moles of phosphoric acid per mole repeat unit].

appears to confirm the important influence of chemical structure on membrane properties in general and proton conductivity in particular. The proton conductivity enhancing mechanism by hydroxy groups is still under investigation, but it is clear that the modification of the chemical structure of PBI membranes increased the proton conductivity even at equivalent acid doping levels. At this point in our studies, two possible mechanisms for conductivity enhancement in 2OH-PBI polymers can be proposed. The first is the direct participation of the hydroxy groups in the proton transport process. Proton conduction in phosphoric acid-based systems is believed to be due to a proton hopping or Grotthuss mechanism that involves the protonation–deprotonation of some species in the membrane. The conductivity enhancement observed in 2OH-PBI containing membranes may simply be due to the increased number of functional groups that can participate in this process. Another possible explanation for the conductivity increase is related to the membrane morphological changes that may occur with different PBI chemical structures. Some preliminary observations of major changes in morphology with PBI structure suggest this could also impact proton conductivity

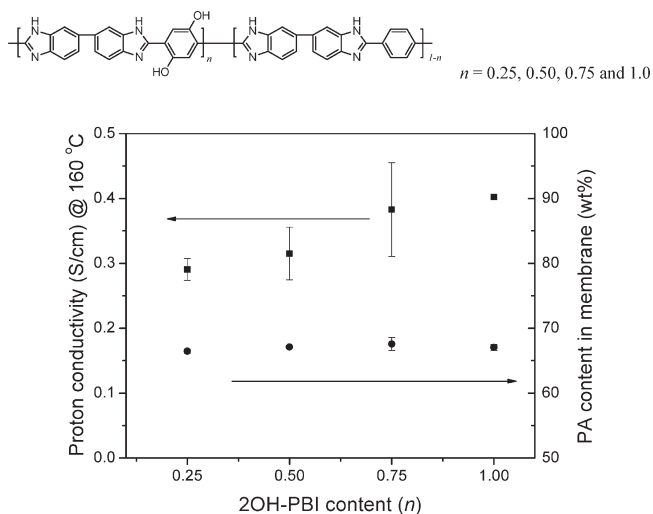


Figure 9. Proton conductivity of 2OH-PBI/*para*-PBI copolymer membranes at 160 °C with different copolymer compositions. Proton conductivity (squares) and PA content (circles). 2OH-PBI [poly(2,2'-(2,5-dihydroxy-1,4-phenylene) 5,5'-bibenzimidazole)], *para*-PBI [poly(2,2'-(1,4-phenylene) 5,5'-bibenzimidazole)].

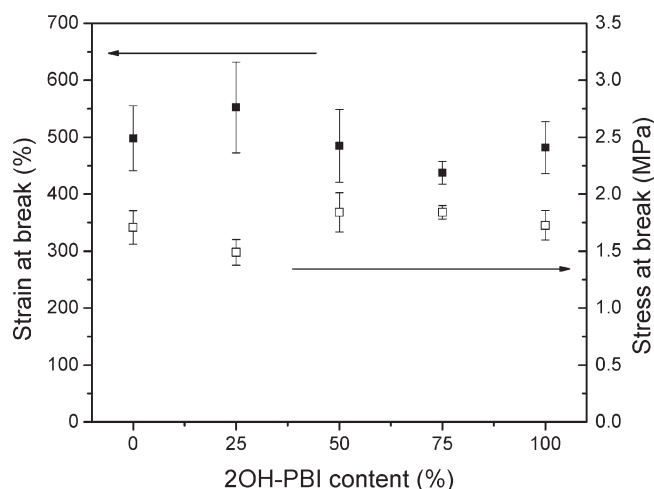


Figure 10. Tensile properties of *para*-PBI [poly(2,2'-(1,4-phenylene) 5,5'-bibenzimidazole)], 2OH-PBI [poly(2,2'-(2,5-dihydroxy-1,4-phenylene) 5,5'-bibenzimidazole)], homopolymers and copolymer membranes. (filled squares: strain at break; unfilled squares: stress at break).

in PPA processed membranes. Currently, more detailed morphology investigations and proton transport studies are being pursued.

Mechanical Properties. The tensile properties of *para*-PBI homopolymer, 2OH-PBI homopolymer, and copolymer membranes were tested at room temperature using an Instron 5843 with samples cut according to ASTM D638 (type V) specifications. As shown in Figure 10, they showed stress at break in the range of 1.49–1.84 MPa and strain at break in the range of 437–552%. Although there was a fluctuation in the mechanical property values, it is difficult to conclude that there is a relationship between polymer compositions and their mechanical properties because the polymerization was stopped after 13 h to prevent the molecular weight growth above the gelation point and optimization of polymerization conditions was not conducted. However, membranes from all polymer compositions showed more than sufficient tensile properties for MEA fabrication and fuel cell testing.

Fuel Cell Performance. The fuel cell performance of 2OH-PBI membranes was investigated with 50 cm² (active area:

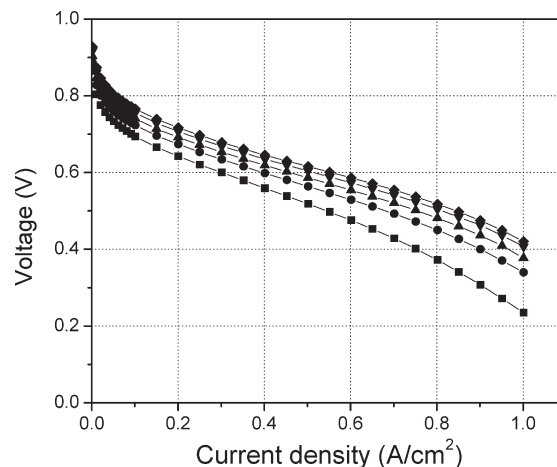


Figure 11. Polarization curves of a 2OH-PBI [poly(2,2'-(2,5-dihydroxy-1,4-phenylene) 5,5'-bibenzimidazole)] membrane based fuel cell at various pressures: 1 mg/cm² Pt/C was used for both cathode and anode electrodes, 160 °C, H₂/air, constant flow (H₂: 415 mL/min; air: 1655 mL/min) [square, 1 atm; circles, 1.5 atm; triangles, 2 atm; down triangles, 2.5 atm; diamonds, 3 atm (absolute pressure)].

45.15 cm²) single stack fuel cells. The fuel cell was prepared using commercially available (E-TEK) platinum (Pt) electrodes (1 mg/cm², 30% Pt on Vulcan XC-72) for both anode and cathode. Figure 11 shows the fuel cell performance of 2OH-PBI at 160 °C under various gas pressures with H₂ and air, Pt catalysts for both anode and cathode. The voltage at 0.2 A/cm², 160 °C was 0.642 V and was approximately the same value as *para*-PBI membranes when measured under the same conditions (~0.64 V at 0.2 A/cm², 160 °C with H₂/air). The voltage gain by raising the gas pressure from 1 to 2 atm was 50 mV, which agrees with increases calculated from experimental data for PAFCs.¹⁵ While the proton conductivity of 2OH-PBI membrane was much higher than that of *para*-PBI membrane as described earlier, the fuel cell performance of 2OH-PBI membrane was approximately the same. The proton conductivity of a membrane is an important factor in determining the fuel cell performance. However, even when the proton conductivity of one membrane is significantly higher than another, the fuel cell performances could be similar due to other limiting factors. Platinum is the most effective material for both hydrogen oxidation and oxygen reduction, but under ordinary conditions, the hydrogen oxidation rate is ~10⁷ times faster than that of oxygen reduction.¹⁶ In PEM fuel cells, the oxygen reduction exchange current density is small, and the polarization on the cathode electrode is the dominant factor in the PEMFC voltage loss.¹⁷ The oxygen reduction reaction (ORR) kinetics is even slower in an acidic medium. The Tafel slopes of the oxygen reduction reaction increased with H₃PO₄ concentration from ~60 mV/decade (up to 5 M) to ~114 mV/decade (14 M) at 25 °C¹⁸ and 110 mV/decade at ~0.9 V in 105% H₃PO₄ at 190 °C.¹⁹ If the slow oxygen reduction reaction rate on the cathode is the limiting factor in determining the overall performance, fuel cell performance might be expected to increase by using better cathode electrodes. There have been extensive efforts to improve the oxygen reduction reaction by modifying the size and the shape of pure Pt catalyst. Another approach to improve the oxygen reduction reaction kinetics is the use of Pt-base bimetallic alloys. Mukerjee et al. showed that binary Pt–M alloy catalysts (M = Ni, Co, Cr) provided a 2–3-fold enhancement of electrocatalytic activities of the ORR relative to pure Pt catalyst under PEMFC operating conditions.²⁰ There have

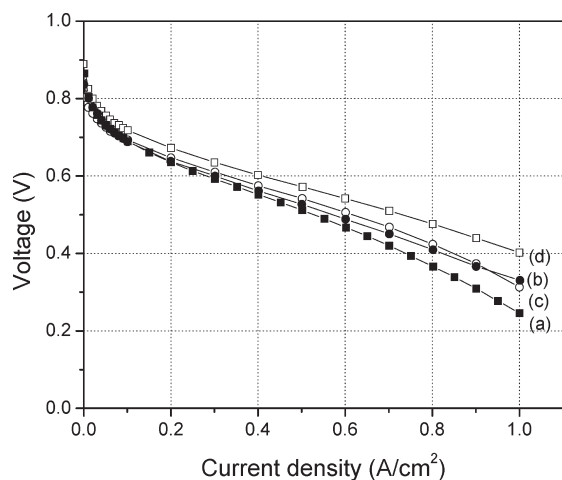


Figure 12. Polarization curves for MEAs containing Pt and Pt alloy catalysts on 2OH-PBI [poly(2,2'-(2,5-dihydroxy-1,4-phenylene) 5,5'-bibenzimidazole)] and *para*-PBI membranes [poly(2,2'-(1,4-phenylene) 5,5'-bibenzimidazole)]. Test conditions: 160 °C, atmospheric pressure (1 atm), constant stoic H_2 ($\lambda = 1.2$)/air ($\lambda = 2.0$), 1 mg/cm² Pt/C for anode electrode [λ , same as defined in Figure 11 caption]. (a) 2OH-PBI membrane, Pt anode/cathode electrodes (filled squares), (b) *para*-PBI membrane, Pt anode/cathode electrodes (filled circles), (c) *para*-PBI membrane, Pt anode catalyst and Pt alloy cathode catalyst electrodes (unfilled circles), and (d) 2OH-PBI membrane, Pt anode catalyst and Pt alloy cathode electrodes (unfilled squares). λ = gas stoichiometric flow, defined as ratio of actual flow of gas delivered to anode or cathode relative to the theoretical rate of gas required.

been many reports that Pt–Ni bimetallic alloy catalysts containing 30–40% Ni significantly enhanced the activity for the ORR.^{21–25}

To evaluate the effect of cathode catalysts, 50 cm² single stack fuel cells were built with 1 mg/cm² Pt/C catalyst on the anode electrode and Pt alloy catalyst on the cathode electrode. Both standard Pt electrodes and Pt alloy electrodes were purchased from E-TEK. Figure 12 shows polarization curves of different types of membranes and cathode catalysts: (a) 2OH-PBI membranes with Pt electrodes for anode and cathode, (b) *para*-PBI membranes with Pt electrodes for anode and cathode, (c) *para*-PBI membranes with Pt electrode for anode and Pt alloy for cathode, and (d) 2OH-PBI membranes with a Pt electrode for anode and a Pt alloy electrode for cathode. Despite the high proton conductivity of 2OH-PBI membranes, the fuel cell performances of 2OH-PBI and *para*-PBI membranes (Figure 12, a and b, respectively) were similar at low current densities and slightly higher for *para*-PBI membranes at higher current densities when standard Pt electrodes were used for both anode and cathode. There was slight improvement in performance with *para*-PBI membranes (Figure 12c) and significant improvement with 2OH-PBI membranes (Figure 12d) when Pt alloy catalyst was used for the cathode. The voltage increase at 0.2 A/cm², 160 °C with H_2 /air was 37 mV, and current density increase at 0.6 V was 120 mA/cm² when the cathode electrode was changed from Pt to Pt alloy cathode electrode with 2OH-PBI membranes. We have previously prepared membranes of much higher proton conductivity that did not exhibit significant increases in fuel cell performance when pure Pt catalysts were used.²⁶ From this limited data, it could be rationalized that slow cathode kinetics might be the limiting factor in fuel cell performance rather than proton conductivity of membranes in 2OH-PBI membrane based fuel cells. Although there was a performance increase when using alloy electrode, it is believed that further improvements in fuel cell performance could be obtained if better electrocatalysts were available.

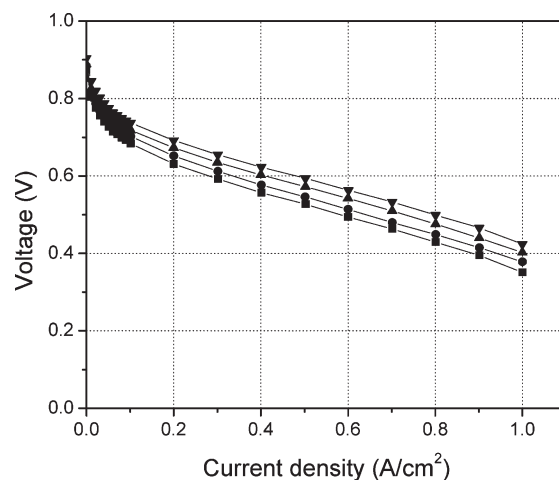


Figure 13. Polarization curves for MEAs using 2OH-PBI [poly(2,2'-(2,5-dihydroxy-1,4-phenylene) 5,5'-bibenzimidazole)] membrane at various operating temperatures: Pt anode electrode, Pt alloy cathode electrode, atmospheric pressure (1 atm), constant stoic H_2 ($\lambda = 1.2$)/air ($\lambda = 2.0$) [λ , defined as in Figure 12 caption] (squares, 120 °C; circles, 160 °C; triangles, 180 °C).

Table 3. Summary of Fuel Cell Performance of 2OH-PBI Membranes Using Different Cathode Electrodes with Reformate/Air at Ambient Pressure^a

entry	temp (°C)	electrode		voltage (V) at 0.2 A/cm ²	current density (A/cm ²) at 0.6 V
		anode	cathode		
1	160	Pt	Pt	0.562	0.131
2	180	Pt	Pt	0.613	0.235
3	160	Pt	Pt alloy	0.648	0.309
4	180	Pt	Pt alloy	0.658	0.369

^a 2OH-PBI [poly(2,2'-(2,5-dihydroxy-1,4-phenylene) 5,5'-bibenzimidazole)].

Figure 13 shows the polarization curves of 2OH-PBI membranes with Pt anode and Pt alloy cathode with H_2 /air operation at different temperatures. The voltage at 0.2 A/cm², 120 °C, ambient pressure was 0.63 V and is comparable to the voltage at 160 °C, ambient pressure when a Pt cathode was used instead of Pt alloy cathode (Figure 11), supporting the previous observation of faster cathode kinetics with Pt alloy catalyst than Pt catalyst. At 180 °C, the fuel cell performance was 0.69 V at 0.2 A/cm² and 0.49 A/cm² at 0.6 V under ambient pressure.

Fuel cell fabrication conditions, measurement conditions, and cell parts were maintained consistently for the data reported in Figures 12 and 13 so it is reasonable to conclude that the fuel cell performance difference between Pt catalyst and Pt alloy catalyst originated mainly from ORR kinetic differences at the cathode catalyst as expected from the previous discussion. Although the quantitative analysis of the effects on fuel cell performance by changing cathode catalyst from Pt to Pt alloy was not available in the literature, linear scan voltammogram results of carbon-supported nanosized Pt and Pt alloy catalysts in 0.5 M HClO₄ saturated with pure oxygen showed that the decrease in overpotential of the ORR on Pt–Ni (2:1)/C catalyst at the same current density is at least 50 mV compared to that on a Pt/C catalyst.²⁴ The fuel cell performance with reformat gas (40% H_2 , 2000 ppm carbon monoxide) and air was also measured at 1 atm. A summary of the reformat fuel cell performance is reported in Table 3 and shows that the performance improvement for alloy catalyst was also significant when reformat gas was used as a fuel.

Conclusions

PBI derivatives having two hydroxy groups per repeat unit were successfully synthesized in poly(phosphoric acid) by lowering the monomer concentration to obtain proper solution viscosity for casting without PA dilution. The cross-linked structure of 2OH-PBI through phosphoric acid ester bridges was confirmed by model compound studies, inherent viscosity studies, and FTIR analysis. The polymerization conditions were adjusted to prevent gelation and allow membrane formation by the PPA process.

2OH-PBI membranes showed higher proton conductivity compared to the unfunctionalized analogue, *para*-PBI membranes. The acid doping level control experiments with 2OH-PBI, *para*-PBI homopolymers, and copolymers showed 2OH-PBI units in polymer chains significantly contributed to the improvement of proton conductivity. This provides evidence that chemical structure of the PBI is an important factor in determining proton conductivity in addition to acid doping level of PBI membranes.

The investigation of the fuel cell performance with Pt and Pt alloy cathode catalysts showed that slow cathode kinetics can be a limiting factor to overall fuel cell performance. The fuel cell performance of 2OH-PBI membranes with Pt alloy cathode catalyst was 0.69 V at 0.2 A/cm² and 0.49 A/cm² at 0.6 V at 180 °C with H₂/air under ambient pressure. Although 2OH-PBI membranes showed higher proton conductivity and improved fuel cell performance with Pt alloy cathode electrode, further study on 2OH-PBI membranes is needed to understand the origin of high proton conductivity.

References and Notes

- (1) Wainright, J. S.; Wang, J. T.; Weng, D.; Savinell, R. F.; Litt, M. J. *J. Electrochem. Soc.* **1995**, *142*, L121–L123.
- (2) Xiao, L.; Zhang, H.; Scanlon, E.; Ramanathan, L. S.; Choe, E. W.; Rogers, D.; Apple, T.; Benicewicz, B. C. *Chem. Mater.* **2005**, *17* (21), 5328–5333.
- (3) Xiao, X.; Zhang, H.; Jana, T.; Chen, R.; Scanlon, E.; Choe, E.-W.; Ramanathan, L. S.; Yu, S.; Benicewicz, B. C. *Fuel Cells* **2005**, *5* (2), 287–295.
- (4) Sikkema, D. J. *Polymer* **1998**, *39* (24), 5981.
- (5) Klop, E. A.; Lammers, M. *Polymer* **1998**, *39* (24), 5987–5986.
- (6) Jenkins, S.; Jacob, K. I.; Kumar, S. *J. Polym. Sci., Part B: Polym. Phys.* **2000**, *38* (23), 3053–3061.
- (7) Tomlin, D. W.; Fratini, A. V.; Hunsaker, M.; Adams, W. W. *Polymer* **2000**, *41*, 9003–9010.
- (8) Tan, L.-S.; Arnold, F. E.; Dang, T. D.; Chuah, H. H.; Wei, K. H. *Polymer* **1994**, *35* (14), 3091–3101.
- (9) Hageman, J. C. L.; van der Horst, J. W.; de Groot, R. A. *Polymer* **1999**, *40* (5), 1313–1323.
- (10) Kosolapoff, G. M. *Organophosphorus Compounds*; John Wiley & Sons, Inc.: New York, 1950.
- (11) Abell, K. W. Y.; Kirby, A. J. *Tetrahedron Lett.* **1986**, *27* (9), 1085–1088.
- (12) Stefani, V.; Souto, A. A.; Acuna, A. U.; Amat-Guerri, F. *Dyes Pigm.* **1992**, *20* (2), 97–107.
- (13) Coates, J. Interpretation of Infrared Spectra, A Practical Approach. In *Encyclopedia of Analytical Chemistry*; Meyers, R. A., Ed.; John Wiley & Sons Ltd.: Chichester, 2000; p 10815.
- (14) Chen, R.; Benicewicz, D. B.; Benicewicz, B. C. In *Electrolyte Concentration Effects in Polybenzimidazole Membranes, Advances in Materials for Proton Exchange Membrane Fuel Cell Systems 2005*, Pacific Grove, CA, Feb 20–23, **2005**.
- (15) *Fuel Cell Handbook*, 6th ed.; EG&G Technical Services, Inc., Science Applications International Corp: 2002.
- (16) Appleby, A. J. *Catal. Rev.* **1971**, *4* (1), 221–244.
- (17) Yu, H.; Yi, B. *Fuel Cells* **2004**, *4* (1–2), 96–100.
- (18) de Sena, D. R.; Gonzalez, E. R.; Ticianelli, E. A. *Electrochim. Acta* **1992**, *37* (10), 1855–1858.
- (19) Maoka, T. *Electrochim. Acta* **1988**, *33* (3), 371–377.
- (20) Mukerjee, S.; Srinivasan, S. *J. Electroanal. Chem.* **1993**, *357* (1–2), 201–224.
- (21) Toda, T.; Igarashi, H.; Watanabe, M. *J. Electrochem. Soc.* **1998**, *145* (12), 4185–4188.
- (22) Drillet, J. F.; Ee, A.; Friedemann, J.; Kotz, R.; Schnyder, B.; Schmidt, V. M. *Electrochim. Acta* **2002**, *47* (12), 1983–1988.
- (23) Paulus, U. A.; Wokaun, A.; Scherer, G. G.; Schmidt, T. J.; Stamenkovic, V.; Radmilovic, V.; Markovic, N. M.; Ross, P. N. *J. Phys. Chem. B* **2002**, *106* (16), 4181–4191.
- (24) Yang, H.; Vogel, W.; Lamy, C.; Alonso-Vante, N. *J. Phys. Chem. B* **2004**, *108* (30), 11024–11034.
- (25) Wakabayashi, N.; Takeichi, M.; Uchida, H.; Watanabe, M. *J. Phys. Chem. B* **2005**, *109* (12), 5836–5841.
- (26) Scanlon, E. Ph.D. Thesis, Rensselaer Polytechnic Institute, Troy, **2005**.